PHYSICAL REVIEW B **81**, 241415(R) (2010)

Electron trapping in misfit dislocations of MgO thin films

Hadj-Mohamed Benia, Philipp Myrach, Anastasia Gonchar, Thomas Risse, Niklas Nilius,* and Hans-Joachim Freund
Fritz-Haber-Institut der MPG, D-14195 Berlin, Germany
(Received 9 June 2010; published 24 June 2010)

Misfit dislocations in a thin MgO/Mo(001) film have been investigated by conductance and light-emission spectroscopy using scanning tunneling microscopy and electron-paramagnetic resonance (EPR) spectroscopy. The line defects exhibit a higher work function than the pristine MgO, being explained by their ability to trap electrons. The electron traps are associated with a nonstoichiometric defect composition in thin oxide films and attractive pockets in the Madelung potential in thicker ones. The latter traps can be reproducibly filled by the adsorption of atomic hydrogen, which gives rise to a free-electronlike signal in EPR spectroscopy.

DOI: 10.1103/PhysRevB.81.241415 PACS number(s): 72.20.Jv, 61.72.Lk, 68.37.Ef, 76.30.Mi

I. INTRODUCTION

The electronic, optical, and chemical properties of wide-gap oxide materials are governed by defects in their crystal structure, e.g., point defects, step edges, and dislocations.[1] Those defects perturb the local oxide stoichiometry, as individual ions or small ion clusters are missing, and give rise to structural relaxations of the surrounding lattice. They also induce discrete electronic states in the band gap that can be filled with electrons. Those extra charges are hold in place by the attractive potential produced by the adjacent ions.[2] The trapping capacity of defects depends on their dimensionality and position in the crystal as well as on modalities of their formation.[3] For example, oxygen vacancies created in an MgO surface by electron bombardment can be filled with one (F^+) or two extra electrons (F^0 center).[4,5] Electron trapping also occurs at morphological peculiarities, such as kinks and reverse corners.[6]

The presence of trapped electrons strongly affects the chemical properties of oxide surfaces. They are involved in the binding of adsorbates either by enabling charge transfer into the adspecies or by facilitating the formation of covalent bonds.[7,8] Gold atoms on MgO(001), as an example, strongly interact with F^+ and F^0 centers, while the binding to electron-depleted F^{2+} sites is negligible.[9] Electron transfer out of the trap may also result in the weakening or breaking of intermolecular bonds if an antibonding orbital becomes filled in this process. The electron-mediated activation of O_2, for instance, is considered to be the key step in various oxidation reactions.[10]

The role of electron traps in the chemistry of oxide surfaces is essentially unknown, and any interrelation between defect density and reactivity proposed in the literature lacks dependable experimental verifications.[8,11] So far, mainly zero-dimensional traps, such as F centers in MgO and CaO, have been characterized by electron-energy loss,[4] optical,[6] electron-paramagnetic resonance (EPR) (Refs. 5, 12, and 13) and scanning tunneling microscopy (STM).[14–16] However, point defects play only a minor role as electron traps due to their small abundance and low storage capacity. In fact, line defects and grain boundaries are the dominant trapping centers in real oxide supports used in catalysis. The large potential of extended defects to trap electrons has been demonstrated in a recent theoretical work by Shluger *et al.*[3] Line defects are also abundant in thin oxide films, being a widely used model system to study catalysis with surface science methods. In such systems, dense dislocation networks develop spontaneously in order to compensate the lattice mismatch with the substrate.[17–19] A systematic characterization of such line defects and the elucidation of their role as electron traps is however missing, mostly because of experimental difficulties to investigate electrically insulating oxide materials. In this STM and EPR study, we demonstrate the trapping ability of misfit dislocations formed in MgO/Mo(001) thin films. Our results show that even well-prepared oxide films are able to capture high numbers of electrons, underlining the general importance of this widely neglected defect type.

II. EXPERIMENT

The experiments are performed in ultrahigh vacuum using an STM operated at 100 K and an X-band EPR machine.[20] The STM is equipped with parabolic mirrors and a spectrograph/charge coupled device detector to monitor photon emission from the tunnel junction. The oxide is prepared by Mg deposition onto a sputtered/flashed Mo(001) surface in 1×10^{-6} mbar O_2 at 300 K. Subsequent annealing to 1100 K leads to the formation of crystalline MgO films, whose surface morphology is governed by the 5% lattice mismatch with the support.[19] Films of 10–15 ML thickness, as used in this study, consist of several 10-nm-wide oxide patches that are slightly tilted against each other. This mosaicity gives rise to distinct crosslike low-energy electron diffraction (LEED) reflexes as shown in Fig. 1(a).[4] The patches are separated by edge dislocations, which often emanate from vertical screw dislocations pinned at the metal-oxide interface. A second kind of line defects are domain boundaries that arise from the coalescence of oxide grains with an out-of-phase crystallographic relation. We will demonstrate in the following that this defect network is able to trap electrons.

III. RESULTS AND DISCUSSION

A first indication comes from a deviating electronic structure of the dislocation lines, as deduced from STM images taken in the field-emission regime [Fig. 1(b)]. At high sample

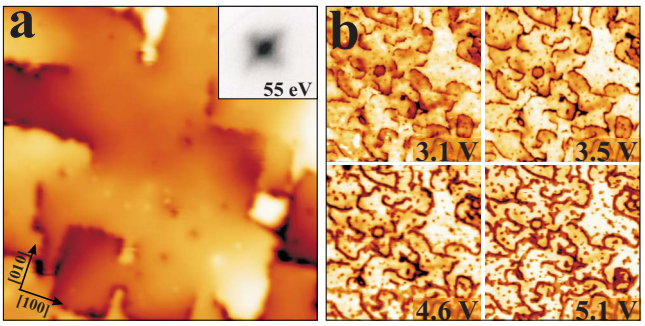

FIG. 1. (Color online) (a) STM image of 12 ML MgO on Mo(001) (3.4 V, 0.05 nA, and 35×35 nm^2). A corresponding LEED pattern is depicted in the inset. (b) High-bias series showing the line defects as deep grooves in the oxide surface (0.05 nA and 100×100 nm^2).

bias, the line defects are imaged with negative apparent height of up to −7 Å compared to the regular film, although the geometric corrugation deduced from low-bias images is below 2.5 Å. The negative contrast indicates a low electron transmissibility of the line defects, forcing the tip to approach the surface in order to maintain a constant current. Electron transport at elevated bias is governed by field-emission resonances (FER), which can be considered as vacuum states that develop in the classical part of a tip-sample junction [Fig. 2(b)].[21] Their energy is defined by the condition that multiples of half the free-electron wavelength fit into the triangular region confined by the tunnel barrier and the sample surface. Quantum mechanically, FER are eigenstates E_n in a triangular potential, the bottom and slope of which are given by the sample work function ϕ and the tip-electric field F, respectively [Eq. 1]: $E_n=\phi+(\frac{3\pi\hbar e\cdot F}{2\sqrt{2m}})^{2/3}n^{2/3}$.[22] As FER carry most of the electron current at high bias, their availability above the MgO surface determines the image contrast in the STM.[16] Apparently, the defect lines offer no or fewer FER than the regular oxide patches and consequently appear dark [Fig. 1(b)]. According

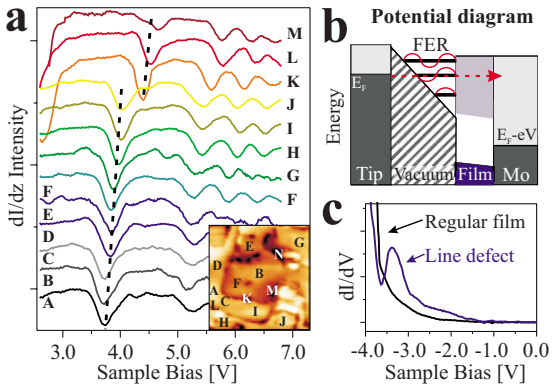

FIG. 2. (Color online) (a) Series of dI/dz spectra measured with enabled feedback loop on terrace (A-J) and defect sites (K-M) of a 12 ML MgO/Mo film. The positions are marked in the inset (0.05 nA and 50×50 nm^2). (b) Visualization of the electron transport through an STM junction in the field-emission regime. (c) dI/dV spectrum taken on a line defect as well as on a defect-free oxide patch.

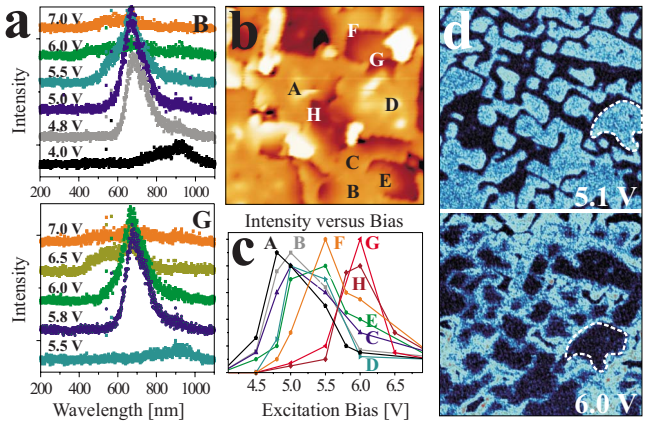

FIG. 3. (Color online) (a) Light-emission spectra taken as a function of excitation bias on a regular terrace site (B) and a line defect (G) (current: 1 nA). The spectral positions are shown in the STM image in (b) (50×50 nm^2). (c) Dependence of the emission intensity on the excitation bias for various surface sites marked in (b). (d) Photon maps (1 nA and 75×75 nm^2) taken at the bias position of the second FER on MgO terraces (top) and defect lines (bottom). The contrast reversal between both images reflects work-function modulations in the film.

to Eq. 1, the energy position of the FER is primarily fixed by ϕ because the tip-electric field is roughly constant in the feedback-controlled imaging mode employed here. The negative contrast, therefore, suggests a work-function increase around the dislocation lines that moves the FER to higher energies. This assumption is confirmed by dz/dV spectroscopy, where the FER show up as minima due to the sudden tip retraction when the next transport channel becomes accessible [Fig. 2(a)]. On defect-free oxide patches (position A-J), the first and second FER are reached around 3.7 V and 5.4 V, respectively, with the exact value depending on the terrace size. Above the line defects, the first and second resonance are systematically upshifted to ~4.4 and ~6.0 V (position K-M), corroborating the local increase in the work function.

Complementary information is obtained from STM light-emission spectra taken on the MgO/Mo films [Fig. 3(a)]. As discussed in earlier work,[23] the optical response is governed by radiative electron transitions from higher to lower FER. The dominant peak at 1.75 eV (700 nm) corresponds to a decay from the second to the first FER while a weak shoulder at 2.5 eV (500 nm) involves the third and first FER. The high cross section of the emission is owed to the long residence time of electronics in the FER being caused by the penetration barrier imposed by the oxide film. Similar to the resonance states, the photon response is sensitive to the oxide work function. On regular MgO terraces, the emission becomes detectable between 4.8–5.5 V excitation bias, which covers the energy window of the second FER in this region [Fig. 3(a)]. In contrast, no emission is observed below 5.8 V for the line defects, in agreement with an upshift of the FER. The energy of the emission peak remains constant in both cases, reflecting the rigid shift of the FER with ϕ. Figure 3(c) summarizes the bias dependence of the photon intensity, as measured for several oxide positions marked in

Fig. 3(b). Whereas on regular patches, the intensity maximum is reached below 5.5 V (position A-E), it shifts above 5.5 V on the line defects (position F-G). This bias difference can be exploited to display the work-function distribution in the MgO film by mapping the integral photon yield as a function of sample bias [Fig. 3(d)]. In photon maps taken at 5.1 V, only the flat MgO terraces with low ϕ emit light and the defects remain dark. The contrast reverses at 6.0 V, as the optical channel opens in the defect regions.

Both, electronic and optical spectroscopy conclusively reveals a work-function increase of ~0.7 eV along MgO/Mo line defects with respect to the regular film. To explain this observation one needs to consider that oxide films in general modify the work function of a metal support. According to density-functional theory (DFT) and Kelvin probe studies, the MgO film reduces ϕ by ~1.5 eV.[24,25] The effect is caused by an electron transfer out of the film that creates a positive interface dipole and the suppressed electron spillout at the metal surface. Surface defects may alter this trend due to their influence on the local charge distribution. While electron-poor defects, such as F^{2+} centers or cationic edge and corner sites produce positive surface dipoles that lower ϕ, electron-rich defects increase the charge density at the surface and hence the work function.[15] The higher ϕ value measured along MgO line defects is therefore compatible with a charge accumulation and indicates electron trapping in the dislocation lines. This conclusion is in agreement with DFT calculations that identified electrostatic pockets in the Madelung potential along an MgO grain boundary that can be filled with electrons.[3,26] The associated gap states are localized close to the conduction-band onset. Due to the high energy of the electrostatic traps, electron trapping will be restricted to oxide films that are sufficiently thick to inhibit electron tunneling into the metal support. Alternatively, a "chemical trapping" of electrons is conceivable. In this case, the excess electrons are captured in the form of reduced Mg^0/Mg^+ species or extra O^{2-} ions and come along with a nonstoichiometric oxide composition along the line defect. As chemical traps are often filled by electron transfer from the metal support, they become active primarily in thin films.

The observed work function increase along the MgO line defects is partly attributed to chemically trapped electrons, as the phenomenon is evident also in films of 2–3 ML thickness.[27] STM conductance spectra reveal a corresponding defect state at −3.3 eV that is absent on the bare film and might accommodate the transfer electrons from the Mo support [Fig. 2(c)]. As the expected deviation from the ideal MgO composition lies only in the percent range, it could not be detected with conventional x-ray photoelectron spectroscopy.[19] In thick MgO films, on the other hand, also the electrostatic traps can be filled, as demonstrated by EPR measurements. After saturating the surface with atomic hydrogen produced by cracking 30 L H_2 on a hot filament, a strong bulklike EPR line develops at $g=2.003$ [Fig. 4(a)]. Its position near the free-electron g value and the lack of the hyperfine signature of hydrogen indicates that the electrons are abstracted from the H atoms as they enter the line defects. The electrons remain however close to the protons, as the EPR line narrows in a characteristic manner upon exchanging H_2 with D_2. The EPR signal is not observed in films below 7 ML thickness, most likely because the electrons are drained to Mo support. It also vanishes when annealing a thick film to 500 K, which indicates thermal activation of the trapped electrons into the MgO conduction band.[28] From this temperature threshold, the energy gap between the trap states and the band onset is estimated to be around 1.0 eV when assuming an attempt frequency of 1×10^{13} s^{-1} for the Arrhenius-type behavior. Such activation energy is in line with the DFT results obtained for MgO grain boundaries.[3] The intensity of the EPR line is compatible with 5×10^{13} unpaired electrons, which provides only a lower bound for the total number of trapped charges. However, already this value is a factor of ten larger than the highest number of electrons that can be stored in paramagnetic point defects.[5] Distributing the trapped charges along the circumference of all dislocation lines, as estimated from the STM images, yields a density of 3–5 electrons per nm line defect. It should be noted that at such high carrier densities electron-electron interactions start to affect the EPR spectra, giving rise to a broadening of the resonance. However, this effect could not be quantified, as the number and distribution of the trapped electrons was not controlled with sufficient accuracy in the experiment.

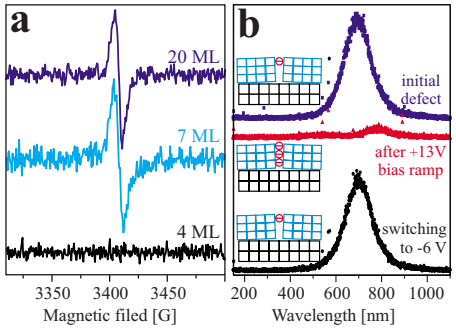

FIG. 4. (Color online) (a) EPR spectra of differently thick MgO/Mo(001) films after exposure to a saturation coverage of H atoms. The bulk signal at $g=2.003$ indicates electron trapping in the line defects of thicker films. (b) Light-emission spectra taken on a pristine line defect (top) after a bias ramp to +13 V (center) and after reversing the polarity (bottom). All spectra are acquired at +6 V sample bias and 1 nA current. The suppressed emission after the ramp is ascribed to electron trapping in the line defect, being reversed at negative bias (see insets).

Filling of the electrostatic traps in thicker films was also achieved locally with the STM. For this purpose, voltage ramps with enabled feedback loop were applied to the STM junction. The effect of electron trapping was then monitored by reversible changes in the optical response. As discussed above, a pristine defect emits photons at 6.0 V excitation bias. After ramping the bias to +13 V and returning to the initial situation, the photon signal vanishes [Fig. 4(b)]. It recovers only after a quick reversal of the bias polarity. Apparently, electrons from the MgO valence band are excited into the shallow trap states at high bias, although those states are not directly accessible for tunneling due to their negligible overlap with the Mo wave functions. The trapped charges trigger a work-function increase that renders the second FER unavailable for optical transitions at 6.0 V excita-

tion bias. The electrons are only stabilized at positive bias but leave the trap states at negative polarity most likely via tunneling to the tip. The subsequent discharging of the gap states restores the initial photon signal. A comparable hysteresis in the optical response is not observed on the oxide terraces, reflecting the crucial role of the line defects in the trapping phenomenon.

In summary, electron trapping in the dislocation network of an MgO/Mo film is concluded from the distinct work-function increase along the oxide line defects, as observed with STM fluorescence spectroscopy. This result is corroborated by a characteristic EPR signal that reflects the presence of unpaired electrons in the trap sites. The defect states that are responsible for electron capturing are of chemical or electrostatic nature. While the former ones fill spontaneously via electron transfer from the Mo support, the latter can be populated via the adsorption of atomic hydrogen or electron injection from the STM tip. In particular, the shallow electrostatic traps are expected to play an important role for the chemistry of the MgO surface, as they may serve as electron donors for adsorbed molecules and metal aggregates.

ACKNOWLEDGMENTS

H.B. and A.G. thank the IMPRS "Complex Surfaces in Materials Science" for financial support. The work has been supported by the COST action D41.

*Corresponding author; nilius@fhi-berlin.mpg.de

[1] H.-J. Freund, Faraday Discuss. **114**, 1 (1999); G. Pacchioni, Solid State Sci. **2**, 161 (2000).

[2] A. L. Shluger, P. V. Sushko, and L. N. Kantorovich, Phys. Rev. B **59**, 2417 (1999); P. Sushko, J. L. Gavartin, and A. L. Shluger, J. Phys. Chem. B **106**, 2269 (2002).

[3] K. P. McKenna and A. L. Shluger, Nature Mater. **7**, 859 (2008).

[4] J. Kramer, W. Ernst, C. Tegenkamp, and H. Pfnür, Surf. Sci. **517**, 87 (2002); J. Kramer, C. Tegenkamp, and H. Pfnür, Phys. Rev. B **67**, 235401 (2003).

[5] M. Sterrer, E. Fischbach, T. Risse, and H.-J. Freund, Phys. Rev. Lett. **94**, 186101 (2005); M. Sterrer, E. Fischbach, M. Heyde, N. Nilius, H.-P. Rust, T. Risse, and H.-J. Freund, J. Phys. Chem. B **110**, 8665 (2006).

[6] T. Berger, M. Sterrer, O. Diewald, and E. Knözinger, J. Phys. Chem. B **108**, 7280 (2004).

[7] V. Nasluzov, V. Rivanenkov, A. Gordienko, K. Neyman, U. Birkenheuer, and N. Roesch, J. Chem. Phys. **115**, 8157 (2001); K. Neyman, N. Roesch, and G. Pacchioni, Appl. Catal., A **191**, 3 (2000).

[8] S. Abbet, E. Riedo, H. Brune, U. Heiz, A. Ferrari, L. Giordano, and G. Paccioni, J. Am. Chem. Soc. **123**, 6172 (2001).

[9] A. Del Vitto, G. Pacchioni, F. O. Delbecq, and P. Sautet, J. Phys. Chem. B **109**, 8040 (2005).

[10] L. M. Molina and B. Hammer, Appl. Catal., A **291**, 21 (2005).

[11] B. Yoon, H. Häkkinen, U. Landman, A. S. Wörz, J.-M. Antoinietti, S. Abbet, K. Judai, and U. Heiz, Science **307**, 403 (2005).

[12] T. Berger, M. Sterrer, O. Diwald, and E. Knözinger, ChemPhys Chem **6**, 2104 (2005).

[13] M. C. Paganini, M. Chiesa, F. Dolci, P. Martino, and E. Giamello, J. Phys. Chem. B **110**, 11918 (2006).

[14] M. Sterrer *et al.*, J. Phys. Chem. B **110**, 46 (2006).

[15] T. König, G. H. Simon, H.-P. Rust, G. Pacchioni, M. Heyde, and H.-J. Freund, J. Am. Chem. Soc. **131**, 17544 (2009).

[16] N. Nilius, Surf. Sci. Rep. **64**, 595 (2009).

[17] M. Klaua, D. Ullmann, J. Barthel, W. Wulfhekel, J. Kirschner, R. Urban, T. L. Monchesky, A. Enders, J. F. Cochran, and B. Heinrich, Phys. Rev. B **64**, 134411 (2001); L. Vassent, M. Dynna, A. Marty, B. Gilles, and G. Patrat, J. Appl. Phys. **80**, 5727 (1996).

[18] J. Schoiswohl, W. Zheng, S. Surnev, M. G. Ramsey, G. Granozzi, S. Agnoli, and F. P. Netzer, Surf. Sci. **600**, 1099 (2006).

[19] S. Benedetti, H. M. Benia, N. Nilius, S. Valeri, and H.-J. Freund, Chem. Phys. Lett. **430**, 330 (2006); S. Benedetti, P. Torelli, S. Valeri, H. M. Benia, N. Nilius, and G. Renaud, Phys. Rev. B **78**, 195411 (2008).

[20] J. Schmidt, T. Risse, H. Hamann, and H.-J. Freund, J. Chem. Phys. **116**, 10861 (2002).

[21] G. Binnig, K. H. Frank, H. Fuchs, N. Garcia, B. Reihl, H. Rohrer, F. Salvan, and A. R. Williams, Phys. Rev. Lett. **55**, 991 (1985).

[22] O. Y. Kolesnychenko, Y. A. Kolesnichenko, O. I. Shklyarevskii, and H. van Kempen, Physica B **291**, 246 (2000).

[23] H. M. Benia, N. Nilius, and H.-J. Freund, Surf. Sci. Lett. **601**, L55 (2007); H. M. Benia, P. Myrach, and N. Nilius, New J. Phys. **10**, 013010 (2008).

[24] J. Goniakowski and C. Noguera, Interface Sci. **12**, 93 (2004); L. Giordano, F. Cinquini, and G. Pacchioni, Phys. Rev. B **73**, 045414 (2006).

[25] T. König, G. H. Simon, H.-P. Rust, and M. Heyde, J. Phys. Chem. C **113**, 11301 (2009).

[26] K. P. McKenna and A. L. Shluger, Phys. Rev. B **79**, 224116 (2009).

[27] H. M. Benia, P. Myrach, N. Nilius, and H.-J. Freund, Surf. Sci. **604**, 435 (2010).

[28] Desorption of H_2 would be an additional explanation for the quenching of the EPR signal at 500 K.